VirusDis. (January–March 2016) 27(1):63–76
DOI 10.1007/s13337-015-0301-9

ORIGINAL ARTICLE

Circulating levels of matrix metalloproteinases and tissue inhibitors of matrix metalloproteinases during Japanese encephalitis virus infection

Vibha Shukla[1] · Akhalesh Kumar Shakya[1] · Mukti Shukla[1] · Niraj Kumari[2] · Narendra Krishnani[2] · T. N. Dhole[1] · Usha Kant Misra[3]

Received: 27 October 2015 / Accepted: 31 December 2015 / Published online: 19 January 2016

Abstract Matrix metalloproteinases (MMPs) are widely implicated in modulating blood brain barrier (BBB) integrity and affect the entry of peripheral immune cells into the central nervous system (CNS). The expression of MMPs is tightly regulated at the level of gene transcription, conversion of pro-enzyme to active MMPs and by the action of tissue inhibitors of metalloproteinases (TIMP). The crucial role of MMPs in inflammation indicates that perturbation of the MMP/TIMP balance decisively plays an important role in pathogenesis during viral encephalitis. The study was performed to evaluate the production of MMP-2, MMP-7, MMP-9, TIMP-1 and TIMP-3 in the sera of JEV i.e. GP 78668A (GP-78) infected BALB/c mouse model of encephalitis and gel zymography was performed for MMP-2 and MMP-9 activities. The estimation of MMP-2, MMP-7, MMP-9, TIMP-1, and TIMP-3 in JEV-infected mouse serum was analyzed by ELISA along with brain histopathology and immunohistochemistry. Evan's blue dye exclusion test was done to check the BBB integrity. Gelatin gel zymography was performed for MMP-2 and MMP-9 activities. We noticed an upregulated expression of MMPs in the sera of virus infected groups compared to controls at different days post inoculation (dpi). Post hoc analysis between days also reveals significant increase ($p < 0.05$) in virus infected groups with disease progression. In contrast, TIMPs expressions were significantly ($p < 0.005$) down regulated in the virus infected group. We provide preliminary evidence for a pattern of TIMP response in JEV infection distinct from that seen in acute inflammatory CNS conditions in JE, shown in our previous findings. Increased MMP-2 and MMP-9 activities were also found in a virus infected group with disease progression and are consistent with our previous finding of MMP-2 and MMP-9 activities in the CNS which clearly demonstrate worsen role of these immune mediators in JEV infection. This study will help to identify new targets for the therapeutic treatment of inflammatory mediated CNS disorders in JEV infection and may lead to the development of potential pharmacological targets in future.

Keywords Japanese encephalitis · Blood brain barrier · Matrix metalloproteinases · Tissue inhibitors of metalloproteinases · Neuropathogenesis · Inflammation

Introduction

Japanese encephalitis virus (JEV) is a neurotropic flavivirus that is spread to humans by infected mosquitoes of Culex sp from non-human vertebrate hosts [14]. The mechanism underlying inflammation and immune responses in Japanese encephalitis (JE) are not fully understood. JEV causes severe damage in the central nervous system (CNS) that includes inflammation and irreparable neuronal loss.

Several neurotropic pathogens have evolved strategies to cross the blood brain barrier (BBB) to gain access to the CNS, including direct infection of BBB cells, paracellular entry through the compromised BBB and transmigration within infected leukocytes via the Trojan-horse mechanism.

Vibha Shukla and Akhalesh Kumar Shakya have contributed equally to this work.

✉ T. N. Dhole
tndhole@yahoo.com

[1] Department of Microbiology, Sanjay Gandhi Post Graduate Institute of Medical Sciences, Raebareli Road, Lucknow 226 014, India

[2] Department of Pathology, Sanjay Gandhi Post Graduate Institute of Medical Sciences, Lucknow, India

[3] Department of Neurology, Sanjay Gandhi Post Graduate Institute of Medical Sciences, Lucknow, India

Increased permeability of the BBB is a pathological hallmark in several neurological disorders such as stroke, multiple sclerosis, bacterial meningitis [20] and neurotropic virus infections including human immunodeficiency virus (HIV) [11], measles virus [10], mouse adenovirus [16] and arthropod-borne viruses such as JEV [28], West nile virus (WNV) [31, 56] and Venezuelan equine encephalitis virus (VEEV) [44]. BBB disruption is associated with the degradation of specific junction proteins, which contributes to virus entry [1] and enhanced transmigration of activated immune cells into the brain [7]. These events correlate with simultaneous production of matrix-degrading enzymes, i.e. matrix metalloproteinases (MMPs), a large family of endopeptidases in the region of injury [40]. In CNS infections, MMPs is thought to play a major role in promoting destructive neuroinflammatory processes, including BBB disruption via TJP degradation, edema formation and disintegration of the neurovascular unit [25, 41].

However, the cellular and molecular mechanism underlying JEV infection in relation to MMPs and tissue inhibitors of metalloproteinases (TIMPs) is largely unknown.

Emerging evidence showed that MMP-9 was involved in BBB eruption, enabling the infiltration of immune cells into the CNS during JE infection [32, 54]. Our previous study [46] also raises the possibility that increased activities of MMP-2 and MMP-9 in CNS worsens the pathology in JEV infection. Pathological activation of MMPs, in particular MMP-9, has been shown to cause a number of detrimental outcomes, including BBB disruption, hemorrhage, neuronal apoptosis [9], and brain damage in ischemic stroke [17] and TBI [18, 33, 60, 61].

Therefore, understanding the key molecular mechanisms by which MMPs modulates inflammation during JEV infection is of utmost importance in the design of effective treatments.

Thus, the present study was aimed to detect the levels of MMP-2, MMP-7, MMP-9, TIMP-1 and TIMP-3 in the serum of JEV infected BALB/c mouse model of encephalitis and mock infected control groups and further investigate the relationship between the levels of MMPs and TIMPs with disease progression.

Materials and methods

Virus strain

An Indian non-neuroinvasive but neurovirulent strain of JEV, GP 78668A (GP-78), a kind gift from Dr. Sudhanshu Vrati, National Institute of Immunology, New Delhi, was used throughout the study. The virus was propagated in the brain of suckling mice. A total of 50 µl from stock was inoculated intracerebrally in 3–4 days old suckling mice. After 4 days, the mice were deeply anesthetized with chloroform and euthanized. Brain were removed aseptically and homogenized in sterile PBS and centrifuged at 13,000 rpm for 30 min at 8 °C. The supernatant was collected, aliquoted and stored at −70 °C till further use. Virus titer was determined by standard plaque assay.

Cell line

Stable porcine kidney cells (PS) were cultured in Eagle's minimum essential media (MEM) supplemented with 10 % fetal calf serum (FCS) [Gibco BRL], penicillin/streptomycin (10,000 U/ml); 100 mg/ml amphotericin B/fungizone and L-glutamine (2 mM) at a constant temperature of 37 °C with 5 % CO_2 [Sanyo, Japan].

Virus titration

Virus titer was measured in the stable porcine kidney cells (PS) by plaque assay as per standard procedure. In brief, PS cell monolayer was grown in 6-well tissue culture plates [Nunc, Denmark]. Tenfold serial dilutions of the propagated virus were made with 2 % MEM. To the 65–70 % confluent PS cell monolayer, 200 µl of each serial dilution was added and adsorbed by frequent shaking for 1 h at 37 °C with 5 % CO_2. Plain MEM was used as a negative control. After adsorption, the cell monolayers were washed with PBS to remove the unadsorbed virus particles. To each well, 3 ml overlay media (a mixture of equal volumes of 1 % agarose (kept at 45 °C) and 2X MEM (kept at 37 °C) was poured and allowed to solidify at RT. The plates were then incubated for 4 days at 37 °C with 5 % CO_2. After 4 days, the cells were fixed by adding 10 % formaldehyde for 2 h at RT. The overlay media were carefully removed and the cells were stained with 1 % crystal violet. Plaques at different dilutions were counted and the dilution showing number of plaques in the range of 20–200 was selected for determination of virus titer using the following formula:

$$\text{Plaque forming units (PFU)/ml} = 1/\text{dilution} \times \text{no. of plaques} \times 1/\text{ml of inoculum/well}$$

Mice strain

Six to eight weeks old inbred female BALB/c mice were used throughout the study. Mice were procured from Industrial and Toxicology Research Center, Lucknow and housed at an animal care facility of our Institute i.e. Sanjay Gandhi Post Graduate Institute of Medical Sciences (SGPGIMS), Lucknow, India. Mice were fed with protein rich diet and water ad libitum. The animals were maintained in an air conditioned room (25 ± 2 °C) with 12-h light (7 a.m.–7 p.m.) and dark cycle. All the experiments were performed during the light

cycle, between 10 a.m. and 2 p.m., and were normalized in all mice. Housing and procedures involving animals and their care were conducted in accordance with the Principles of Laboratory Animal Care (National Institutes of Health Publication Number 86-23, revised 1996). The study was approved by the local ethics committee, and all the experiments were carried out in accordance with the institutional guidelines on the care and use of experimental animals.

Mice inoculation and sacrifice schedule

Twenty four BALB/c mice were included in the study. Twelve mice were infected with JEV (GP-78) of 3×10^6 Plaque forming units (PFU) by intra-cerebral route (IC). Sterile phosphate buffered saline (PBS) was inoculated into rest 12 mice (age and sex matched controls) by IC route. Mice were monitored daily for signs, symptoms of encephalitis and survival. Blood samples were collected by retro-orbital route at 1, 2, 3, 4, 5 and 6 days post inoculation (dpi) for RNA extraction to see virus multiplication in the serum at each day after JEV infection from Real time RT-PCR. But MMPs and TIMPs expression by ELISA were seen only in the serum at 1, 3, 5 and 6 dpi to investigate whether the increased expression of MMPs (−2, −7, −9) and TIMPs (−1, −3) in the CNS of JEV infected BALB/c mouse model [46] with disease progression and brain tissue pathology is mirrored or not in the peripheral venous blood.

At each time point, three mice each from both control and virus-infected groups were selected. Brain was excised aseptically and stored at −80 °C for future study.

Quantitative real time RT-PCR

RNA was extracted using the QIAamp Viral RNA Mini Kit (QIAGEN) from serum samples according to the manufacturer's instruction. To detect and quantify the JEV RNAs, commercially available kit (Genome diagnostic) was used according to the manufacturer's instruction. Primers were specific for a 130 bp region of the JEV envelope gene. The probe was labeled with the reporter dye FAM at the 5′ end and the quencher dye TAMRA at the 3′ end. The reaction condition was 50 °C for 15 min, 95 °C for 10 min, 45 cycles of 94 °C for 10 s, 55 °C for 20 s, and 72 °C for 15 s, using the ABI 7500 Real Time PCR System (Applied Biosystems, Foster City, CA, USA). Water (PCR grade) was used as a negative control. This kit was already used by an Indian author for virus quantitation [5].

Enzyme-linked immunosorbent assays for MMPs and TIMPs

The total MMP-9, TIMP-1 (Quantikine R&D system, Minneapolis, Minn; USA), MMP-2, MMP-7, and TIMP-3 (USCN Life Science Inc. Wuhan, P. R. China) concentrations was determined in the serum of virus infected mice groups and mock infected controls using commercial ELISA kits. All samples were measured in triplicate. According to the manufacturer's recommendations, the serum samples were diluted using assay buffer. Standard curves were prepared as per the instructions given along with the kits. The MMPs and TIMPs levels were expressed as pg/ml.

Detection of MMP-2 and MMP-9 activities by gel zymography

Sodium dodecyl sulfate–polyacrylamide gel electrophoresis (SDS-PAGE) zymography was performed to determine gelatinase activity as described by Kieseier et al. [22]. Briefly, the concentration of protein was measured using a Bio- Rad protein assay Kit (Bio-Rad, Hercules, CA). Ten fold diluted sera having 20 μg of total proteins were separated on the 10 % precast zymogram (Novex, San Diego, Calif., USA) at 125 V for 1.5 h under non reducing conditions of 5X non reducing loading buffer, 0.4 M Tris–HCL (pH 6.8), 20 % glycerol, 5 % sodium dodecyl sulfate, and 0.1 % bromophenol blue, followed by 1 h of incubation (three times, 20 min each) in 2.5 % Triton X-100 (Sigma, St. Louis, MO) and incubation for 16 h in 1X zymogram developing buffer (Novex) for the development of enzyme activity bonds. After incubation, the gels were stained with 0.5 % Coomassie Brilliant Blue G-250 (Hi-Media, Mumbai, India) in a mixture of methanol: acetic acid: H2O (50:10:40). The gelatinase activities were detected as unstained bands on a blue background, representing areas of gelatin digestion. The images were captured and analyzed using the Gel documentation system (BioRad ChemiDoc XRS, USA). A representative gel was chosen for each experiment, and band densities were analyzed by densitometric scanning software Image Quant TL (GE-Pharmacy Biotech). The results at each time point were expressed as mean ± SD values.

Assay of blood brain barrier (BBB) integrity

BBB integrity was evaluated by Evan's blue dye exclusion test [2, 27]. Mice were grouped as described above, i.e. control group and JEV infected group. A total of three mice each from control and JEV infected group (IC injection) at each time points, i.e. 1, 3, 5 and 6 dpi was injected intravenously with 75 μl of 2 % Evan's blue (Sigma) in PBS. One hour later, mice were sacrificed and transcardially perfused with 10 ml of normal saline. Brains were then removed and photographed.

Histology and immunohistochemistry (IHC)

Histopathology and IHC of brain tissues were carried out in the Department of Pathology, SGPGIMS, Lucknow, India.

The mice were anesthetized with ether and perfused with 150 ml PBS (0.1 M, pH 7.2). The brain were sliced and fixed in 10 % buffered formalin for 3 days. After fixation the tissues were sectioned in 3–5 mm slices and processed overnight. Next day, the tissues were embedded in paraffin blocks. Five micron section was cut and dewaxed in xylene and graded alcohol (absolute 90, 70 %) and brought to water. One section of each block was cut and stained with hematoxylin-eosin (HE). Histopathological evaluation was done by the experienced pathologist. The pathologist who was evaluating the sections was blinded for the treatment group.

For IHC, the sections were cut and lifted on polylysine coated slides and brought to water as above. Antigen retrieval was done in citrate buffer for half an hour at 98 °C and pH 6.0. Endogenous blocking was done by 3 % H_2O_2 and washed in between with TRIS buffered saline. Primary antibody (clone NS1 for JEV protein detection at 1:25 dilution from Abcam, USA; MMP-2 & MMP-9 at 1:40 dilution from Novocastra, UK) was applied for 2 h at room temperature and washed with TRIS buffered saline. Then, Secondary antibody (Universal Envision, DAKO) was applied for 30 min and then washed with TRIS buffered saline and then treated with a chromogen (Diaminobenzidine). The slides were counterstained with hematoxylin and mounted with DPX.

Statistical analysis

All the statistical analysis was done by using SPSS statistical software version 15.0 (SPSS Inc, Chicago, IL.USA). Student—t test for independent groups was performed to compare the MMPs and TIMPs levels between mock infected control and virus infected mice. Differences in the expression with the time course were analyzed by using one way analysis of variance (ANOVA) followed by Post-hoc multiple comparison analysis using Scheffic's test. Correlation analysis between serum MMPs and TIMPs level, between serum MMP-2 and MMP-9 activities was done using Pearson's coefficient of correlation (r). Relationship of MMP-2 and MMP-9 with viral transcript was done using regression analysis (R^2). A p value of ≤ 0.05 was considered statistically significant.

Results

Mice survival and clinical signs and symptoms

All the mice in the mock infected controls were healthy with no clinical sign and symptoms at any time point. In the virus infected mice, 100 % mortality was observed after 7 dpi. Thus, we have chosen time point up to 6 dpi in our study group. In the virus infected group, hunching of the back and slight hind limb disability was observed on 4 dpi. The typical symptoms of encephalitis characterized by total hind limb paralysis, tremors, and convulsions with altered consciousness became evident on 5 and 6 dpi.

Virus load in sera of JEV infected (IC) mice

RNA was extracted from the sera of mice at each dpi (i.e. 1, 2, 3, 4, 5, and 6) both in the control group and virus infected group, and the number of JEV copies was quantified by real time RT-PCR by comparison with a standard curve drawn from titrated JEV RNA transcripts (provided by the kit Genome diagnostic). In the control group no virus was detected at all the time point. While in virus infected group, no virus was detected at 1 dpi. At 2dpi, 2×10^6 copies/ml was observed, which subsequently increased to 3.6×10^7 copies/ml at 3 dpi and 3.8×10^7 copies/ml at 4 dpi respectively. The JEV copies at 5 dpi was almost same as 4 dpi, i.e. 3.3×10^7 copies/ml and at 6 dpi decreased JEV copies was observed i.e. 2.7×10^6 copies/ml. The possible reason for decrease in virus load in serum at later stages of infection may be due to the activation of immune response [43, 49] in the peripheral system. There is a possibility that the virus may be eliminated by the host's immune system in the later stage by neutralizing antibodies and cellular immunity.

MMPs and TIMPs serum concentrations in JEV infected mice groups and mock infected controls

MMP-2, MMP-7, MMP-9, TIMP-1 and TIMP-3 were assessed at 1, 3, 5 and 6 dpi in the blood collected from eye bleeding of both mock and virus infected groups of mice. The results were expressed as mean ± SD values of MMPs and TIMPs in JEV infected mice groups and mock infected controls.

MMP-2

In the controls, the total MMP-2 concentration was 192.116 pg ± 0.006 pg, where as in the virus infected mice serum MMP-2 concentration was found to be 206.590 pg ± 0.519 pg at 1 dpi and peaked onwards at 5 dpi 268.798 pg ± 0.045 pg and at 6 dpi 271.198 pg ± 0.002 pg. The level of MMP-2 in the virus infected group was significantly higher ($p < 0.001$) at all dpi compared to controls. A significant increase ($p < 0.001$) was observed in the virus infected group at 3 dpi compared to 1 dpi which further increased significantly ($p < 0.001$) at 5 dpi compared to 3 dpi and at 6 dpi compared to 5 dpi (Fig. 1a).

MMP-7

In the controls, the MMP-7 level was 3711.437 pg ± 1.821 pg, whereas in the virus infected group it was 4304.187 pg ± 4.175 pg at 1 dpi which increased onwards and at 6 dpi the MMP-7 level was 6907.789 pg ± 56.988 pg. In the virus infected group, the MMP-7 level was significantly higher ($p < 0.001$) at all dpi compared to controls. A significant increase ($p < 0.001$) was also observed in the virus infected group at 3 dpi compared to 1 dpi with a further significant increase ($p < 0.001$) at 5 dpi compared to 3 dpi, although at 6 dpi increase in the MMP-7 level was not significant ($p = 0.08$) compared to 5 dpi (Fig. 1b).

MMP-9

In the controls, MMP-9 level was 101.198 pg ± 0.605 pg whereas in the virus infected group, it was 115.227 pg ± 0.026 pg at 1 dpi and peaked to 218.387 pg ± 0.771 pg at 5 dpi and 229.01 pg ± 8.027 pg at 6 dpi. In the virus infected group, the MMP-9 level was significantly higher ($p < 0.001$) at all dpi compared to controls. A significant increase ($p < 0.001$) was also observed in the virus infected group at 3 dpi compared to 1 dpi, with a further significant increase ($p < 0.001$) at 5 dpi compared to 3 dpi, although at 6 dpi increase in the MMP-9 level was not significant ($p = 0.007$) compared to 5 dpi (Fig. 1c).

TIMP-1

In the controls, TIMP-1 level was 2944.097 pg ± 39.178 pg, whereas in the virus infected group, a very high level of TIMP-1 was observed at 1 dpi i.e. 7706.208 pg ± 5.204 pg, 3 dpi i.e. 6479.229 pg ± 19.699 pg and at 5 dpi i.e. 5106.609 pg ± 8.161 pg compared to controls. TIMP-1 level was decreased from 1dpi onwards and at 6 dpi; low level of TIMP-1 was detected i.e. 3494.539 pg ± 3.834 pg with disease progression in the virus infected group. The decrease in the level of TIMP-1 was significant ($p < 0.001$) in the virus infected group compared to controls at all dpi. A significant decrease ($p < 0.001$) was observed in the virus infected group at 3 dpi compared to 1 dpi which further decreased significantly ($p < 0.001$) at 5 dpi compared to 3 dpi and at 6 dpi compared to 5 dpi (Fig. 1d).

TIMP-3

In the controls, TIMP-3 level was 14.169 pg ± 0.069 pg, whereas in the virus infected group, likewise,TIMP-1 a very high level of TIMP-3 was observed at 1 dpi i.e. 28.894 pg ± 0.019 pg, 3 dpi i.e. 26.937 pg ± 0.064 pg and at 5 dpi i.e. 22.173 pg ± 0.057 pg compared to controls. TIMP-3 level was decreased from 1 dpi onwards and at 6 dpi; low level of TIMP-3 was detected i.e. 12.431 pg ± 0.037 pg with disease progression in the virus infected group. The decrease in the level of TIMP-3 was significant ($p < 0.001$) at all dpi compared to controls. Decrease in level was also significant ($p < 0.001$) between the entire dpi in the virus infected group (Fig. 1e).

Detection of MMP-2 and MMP-9 activities in sera by gel zymography

Gel zymography was performed to ascertain the gelatinase activities of MMP-2 and MMP-9 in JEV infected mouse brain. In the controls, MMP-2 activity was 906.007 µg ± 2.000 µg, whereas in the virus infected mice, increased MMP-2 activity was found to be 2796.029 µg ± 75.102 µg at 1dpi and 5780.645 µg ± 73.259 µg at 3 dpi which further peaked at 5 dpi 7038.870 µg ± 57.709 µg and at 6 dpi 9383.619 µg ± 164.731 µg compared to controls (Fig. 2a). MMP-2 activity in the virus infected group was significantly higher ($p < 0.001$) at all dpi compared to controls. A significant increase ($p < 0.001$) was observed in the virus infected group at 3 dpi compared to 1 dpi which further increased significantly ($p < 0.001$) at 5 dpi compared to 3 dpi and at 6 dpi compared to 5 dpi (Fig. 2a). Similarly, in the controls, MMP-9 activity was 249.000 µg ± 1.000 µg where as in the virus infected group, marked increased was noticed at 1 dpi i.e. 2025.042 µg ± 12.439 µg and peaked to 3072.071 µg ± 55.253 µg at 5 dpi and 3632.084 µg ± 48.636 µg at 6 dpi (Fig. 2b) as compared to controls. In the virus infected group, MMP-9 activity was significantly higher ($p < 0.001$) at all dpi compared to controls. A significant increase ($p < 0.001$) was observed in the virus infected group at 3 dpi compared to 1 dpi which further increased significantly ($p < 0.001$) at 5 dpi compared to 3 dpi and at 6 dpi compared to 5 dpi (Fig. 2b). The increased activity of MMP-2 and MMP-9 in sera was associated with disease severity when compared with controls.

Correlation analysis of the serum MMPs and TIMPs level in virus infected mice groups

To determine the coefficient of correlation between each variable (MMP-2, MMP-7, MMP-9, TIMP-1 and TIMP-3 serum level), Pearson's coefficient of correlation was determined by pairing each variable with another. Relationships between MMPs and TIMPs are shown in Table 1. The analysis indicates a strong correlation between the expression of MMPs and TIMPs.

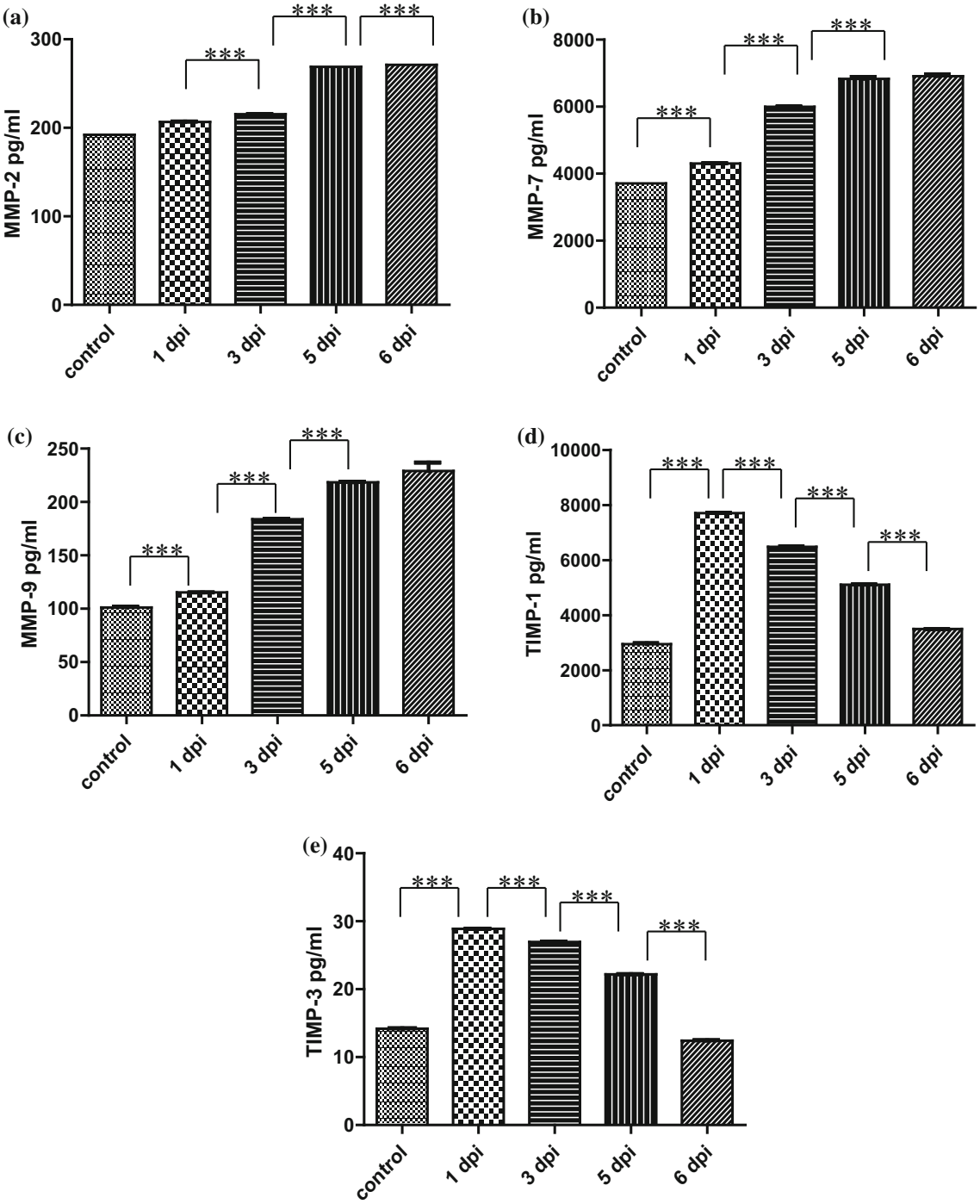

Fig. 1 *Bar diagrams* showing MMPs and TIMPs levels at different time points in serum of mock infected control mice and JEV infected mice. **a** Levels of MMP-2 **b** Levels of MMP-7 **c** Levels of MMP-9 **d** Levels of TIMP-1 **e** Levels of TIMP-3. Values are mean ± SD of 3 animals in each of the 1, 3, 5, 6 dpi and control groups. One way ANOVA; $p < 0.05$ is considered significant (*$p < 0.05$; **$p < 0.01$; ***$p < 0.001$)

Relationship of MMP-2 and MMP-9 expression in sera with virus transcript

The relationship between viral transcript and expressed protein concentration of MMP-2 and MMP-9 in the virus infected mice in serum was observed by simple linear regression analysis (Fig. 3). Although MMP-2 and MMP-9 serum concentration increases from 1 dpi to 6 dpi there was a moderate relationship found in virus transcript ($R^2 = 0.640$, $p = 0.001$; $R^2 = 0.590$, $p = 0.001$ respectively).

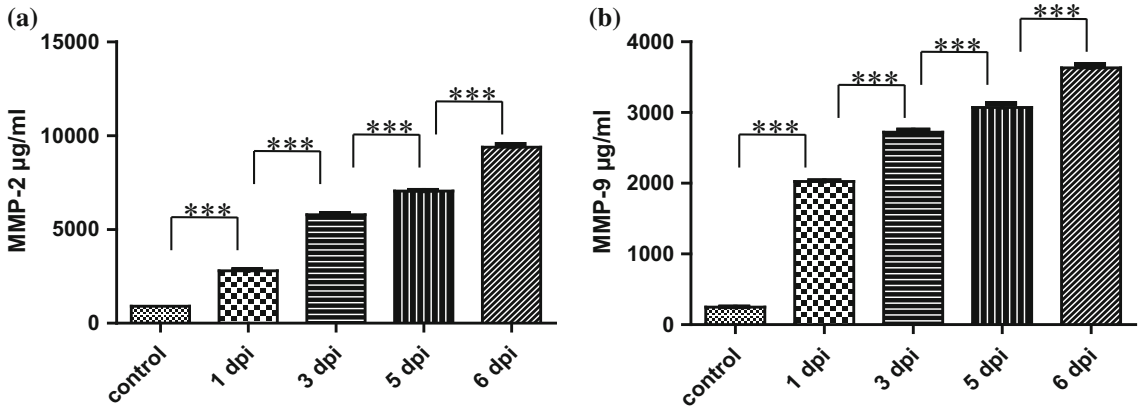

Fig. 2 Zymography analysis of MMP activities in serum of mock-infected control and JEV-infected mice at different time points. **a** MMP-2, **b** MMP-9. Values are mean ± SD of 3 mice in each of the 1, 3, 5, and 6 dpi and control groups. One way ANOVA; $p < 0.05$ is considered significant ($*p < 0.05$; $**p < 0.01$; $***p < 0.001$)

BBB damage in mice infected with JEV

Evan's blue is a cationic dye that binds to serum albumin to form a dye- protein complex that cannot pass through the intact BBB. Due to this, it is used as a standard molecule to test the permeability of the BBB [30]. Intravenous injection of Evan's blue results in the formation of a conjugate with serum albumin. Inclusion of the blue colored dye in the brain indicated the passage of the dye protein conjugate into the brain that signifies increased permeability or damage of BBB. In the present study, mice from the control group and JEV infected group were taken at each time point to test the BBB permeability (Fig. 4). The marked leakage of Evan's blue dye in the JEV infected mouse brain at 3 and 5 dpi indicates the compromised BBB integrity with respect to control.

Histopathology

Section of mouse brain stained with HE showed neuronal damage in the form of neuronal shrinkage and hyper eosinophilia. There was edema, spongy degeneration and infiltration by neutrophil and lymphocytes within the brain parenchyma around neurons more in the thalamic and hypothalamic area followed by the cerebral cortex. Perivascular inflammatory infiltrate was seen. Cerebellum showed only mild neuronal damage displaying shrinkage and hyper eosinophilia (Figs. 5, 6). These changes in the brain parenchyma were appreciable at 5th dpi and were more intense on 6th dpi.

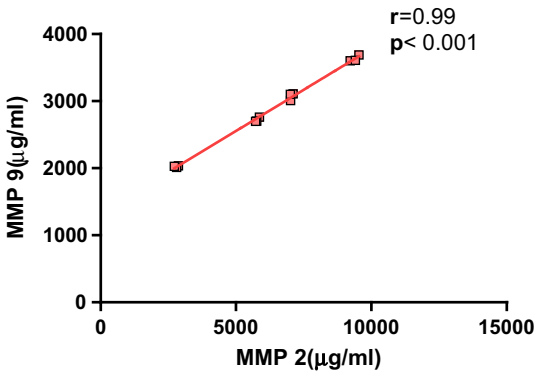

Fig. 3 Correlation analysis between MMP-2 and MMP-9 activities in serum of JEV infected mice

Table 1 MMPs and TIMPs level in sera of mock infected controls mice and JEV infected mice at different time points

Variables	Controls	JEV infected mice			
	Mice	1 dpi	3 dpi	5 dpi	6 dpi
MMP-2	192.116 ± 0.006	206.590 ± 0.519	215.495 ± 0.016	268.798 ± 0.045	271.198 ± 0.002
MMP-7	3711.437 ± 1.821	4304.187 ± 4.175	5997.481 ± 6.545	6832.966 ± 56.877	6907.789 ± 56.988
MMP-9	101.198 ± 0.605	115.227 ± 0.026	183.927 ± 0.385	218.387 ± 0.771	229.01 ± 8.027
TIMP-1	2944.097 ± 39.178	7706.208 ± 5.204	6479.229 ± 19.699	5106.609 ± 8.161	3494.539 ± 3.834
TIMP-3	14.169 ± 0.069	28.894 ± 0.019	26.937 ± 0.064	22.173 ± 0.057	12.431 ± 0.037

Values (pg/ml) are expressed as mean ± SD of 3 mice in each group

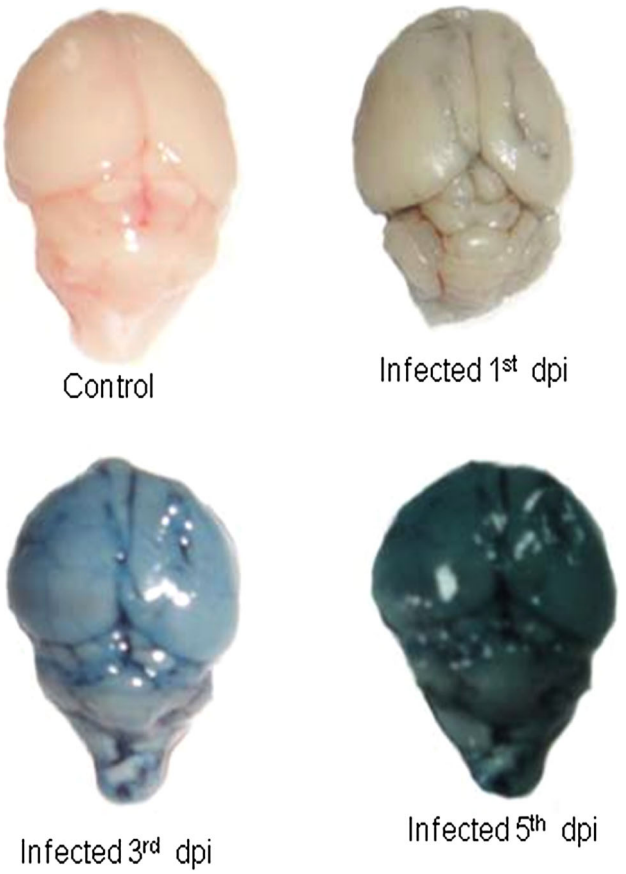

Fig. 4 Blood brain barrier damage of mice infected with JEV (IC challenge) by Evan's blue dye exclusion test

IHC

IHC was performed to look for the presence JEV antigen. Our IHC results showed JEV infected neurons in the hypothalamus, thalamus and cortex. Cerebellum neurons did not show the presence of JEV NS1 antigen. The antigen was first visible at 5th day post infection and more pronounced on the 6th day post infection (Fig. 7). IHC was also performed to look for the presence of MMP-2 & MMP-9 proteins in JEV infected mouse brain. Staining with specific antibodies showed MMP-2 and MMP-9 positive neurons in the cortex of JEV infected mouse brain compared to control mice (Fig. 8).

Disscusion

To examine whether the increased expression of MMPs (−2, −7, −9) and TIMPs (−1, −3) in the CNS of JEV infected BALB/c mice model [46] is mirrored in the peripheral venous blood, this time we studied the expression of these specific MMPs and TIMPs in the mice sera by ELISA. It has also been reported that the immune response to viral infection of CNS differs from that in the periphery, because of the potentially damaging consequences of cellular cytotoxicity, altered vascular permeability and the influx of inflammatory cells into the brain [26].

Our previous study [46] demonstrated that at initial stages i.e. at 1 and 3 dpi of IC JEV infection, where no clinical signs of disease or mortality were observed, the expression of MMPs and TIMPs were found to be significantly increased with increasing virus load and increased tissue damage characterized by inflammatory cell infiltrations in brain parenchyma, perivascular cuffing and at the later stages, tissue necrosis.

Immunohistochemical report suggests that the JEV NS1 antigen was localized in the thalamus, mid brain, hypothalamus and cerebral cortex at 5th dpi and it was observed that JEV antigen was more pronounced at 6th dpi in all the regions studied. The presence of MMP 2 and MMP-9 positive neurons was observed in the cortex region of JEV infected mouse brain when stained for these two specific proteins.

The MMP 2 and MMP-9 are known to cause BBB disruption by degrading collagen IV, its main component [41], interferon (IFN)-α, a potent antiviral cytokine and microglial activator [38], and tumor necrosis factor (TNF)-α which has been shown to directly activate microglia [3] and induce neuronal apoptosis [32]. The MMP levels have been shown to correlate with the severity of some CNS infections [24]. The critical role of MMPs & TIMPs in the pathology of JE was also supported by our recent clinical studies [20], in which higher concentrations of MMP-2, TIMP-2 and TIMP-3 in cerebrospinal fluid (CSF) and serum of children with JEV infection was noticed compared with disease control. Higher TIMP-1 concentration in CSF was observed in a JEV infection group compared to disease control. Also a higher concentration of MMP-9 and MMP-7 was observed in the serum of children with JEV infection when compared with disease control and healthy control but not in CSF.

In humans an elevated concentration of MMPs in serum/CSF correlated with disease severity [51]. Based on published literature, it is suggested that MMPs could be a key target in future to be used as therapy, by attenuating the inflammatory cascades responsible for brain damage during JEV infection.

BBB disruption is potentially related to MMP activity [41]. In JEV infection, MMPs might play a detrimental role by degrading BBB. TNF-α and IL-1β is a well-recognized stimulator of MMP-9 production [39]. We hypothesized that in JEV infection, MMP contribute to neuronal destruction via stimulation of TNF- α release. Expression of MMP-9 can be induced by extracellular stimuli at the transcriptional and translational levels [19, 57]. Many reports have shown

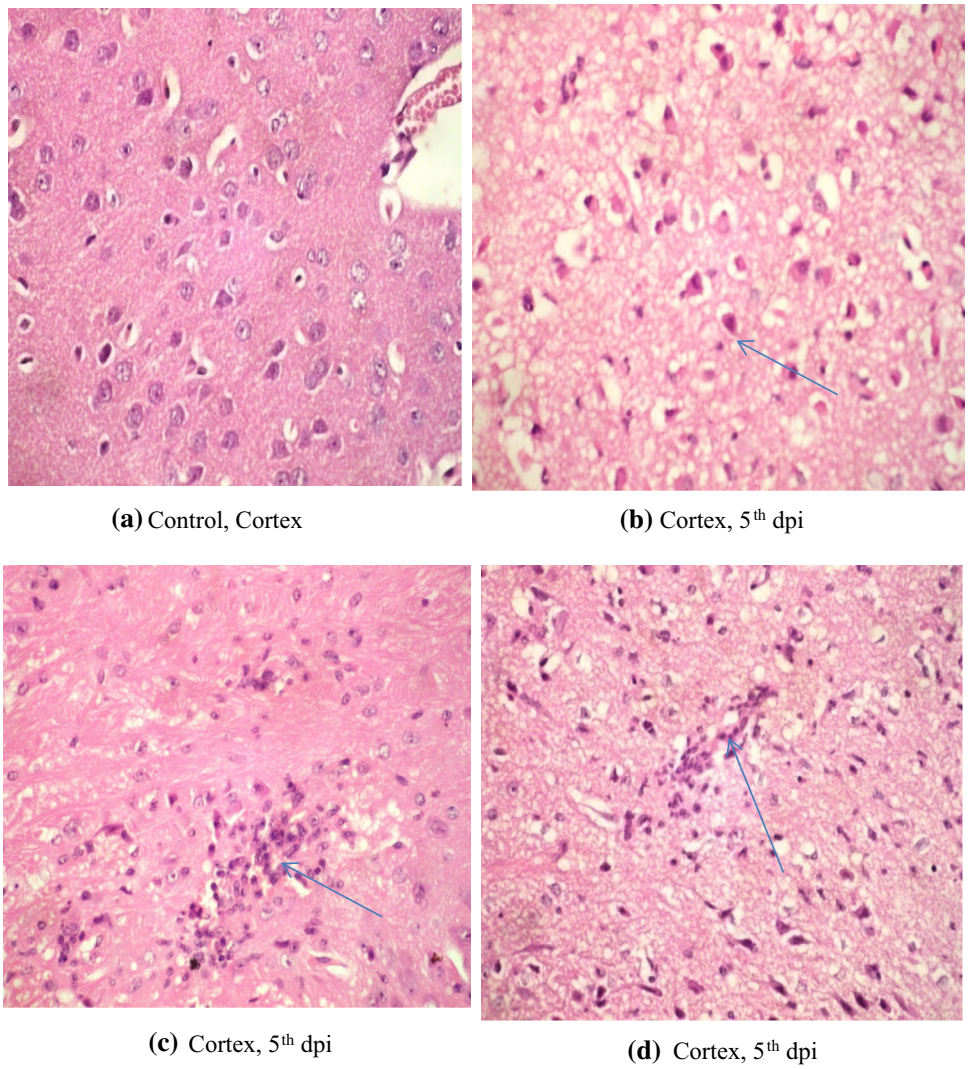

(a) Control, Cortex

(b) Cortex, 5th dpi

(c) Cortex, 5th dpi

(d) Cortex, 5th dpi

Fig. 5 Photomicrograph of H & E staining showing **a** normal appearing neurons with round nuclei, vascular chromatin, prominent nuclei and moderate cytoplasm in cortex of control mice brain, **b** neuronal shrinkage with shrunken nuclei and hypereosinophilic cytoplasm, **c** inflammatory cell infiltrate with in the brain parenchyma causing neuronal damage, **d** perivascular inflammatory cells and neuronal damage at 5th dpi (Magnification at ×40)

that the promoter of MMP-9 possesses a series of functional activator/enhancer element binding sites, including NF-κB and activator protein-1 (AP-1) [41, 59]. Upregulation of MMP-9 by viral infection has been shown to trigger tissue injury in various organs. For instance, the GP 120 protein of the human immunodeficiency virus (HIV) disrupts the BBB by increasing MMP-9 and reducing vascular tight junction proteins via mechanisms involving ROS generation and oxidant injury [21, 30].

This time we determined the serum levels of MMPs and TIMPs in mock infected controls and virus infected mice at different day post inoculation i.e. 1, 3, 5 and 6 dpi. The study shows, MMP-2, MMP-7 and MMP-9 levels were upregulated in the mice sera after IC JEV challenge, while TIMP 1 and TIMP3 levels were substantially down regulated with the disease progression. The mean serum MMP-2 and MMP-9 level was found to be peaked significantly ($p < 0.001$) at 5dpi and 6dpi in the virus infected mice group compared to controls with disease progression. The mean MMP-7 serum concentration was also increased significantly ($p < 0.001$) at all dpi and peaked at 3 dpi and 5 dpi compared to controls. Multiple comparison analysis in the virus infected group showed significant ($p < 0.001$) increased serum MMP concentration with disease progression.

Rises in serum MMPs may represent peripheral T cell activation. Transmigration of pathogenic T cells across the BBB is facilitated by the expression of cell adhesion molecules and proteases that degrade the ECM [36]. Our present findings are consistent with the hypothesis that raised MMP-9 levels play a role in a BBB breakdown in vivo and are consistent with our previous findings [20] of increased MMP expression/activities in CNS of BALB/c mice model challenged with JEV with disease development and tissue pathology and increased levels of MMPs in CSF and serum compared to healthy controls in our earlier clinical studies [47]. MMP-9 in the CSF has been proposed as a marker of meningitis, neurotropic viruses and neuroinflammation [37, 52, 53].

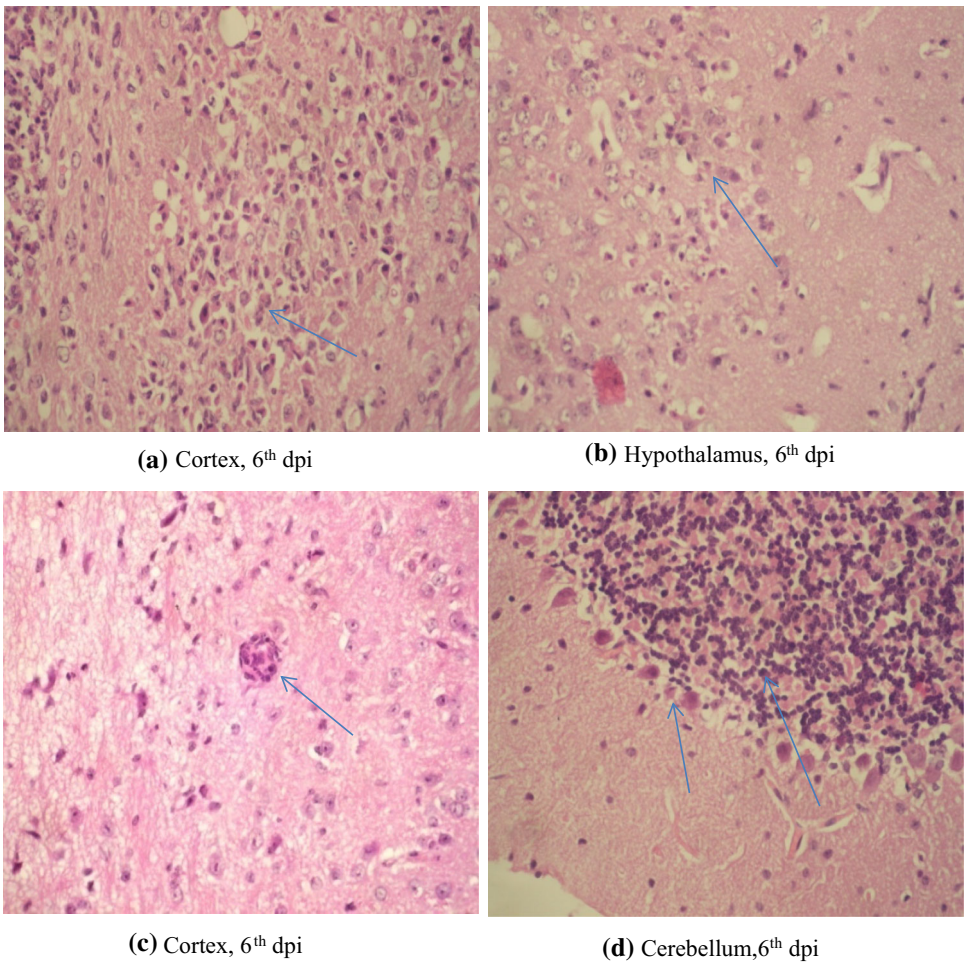

(a) Cortex, 6th dpi

(b) Hypothalamus, 6th dpi

(c) Cortex, 6th dpi

(d) Cerebellum,6th dpi

Fig. 6 **a** Intense inflammatory infiltration causing necrosis of brain parenchyma, **b** Inflammatory infiltrate and neuronal damage, **c** Perivascular inflammation in the cortex, **d** Cerebellum showing neuronal shrinkage & hypereosinophilia of the purkinjee cells at 6th dpi (Magnification at ×40)

In a study by Dutta et al., [20], it has been demonstrated that MMP-9 has significant role in damaging the barrier in JEV infection [29]. Moreover previous study by Tung et al. [54] demonstrated that JEV induces expression of MMP-9 that causes brain damage in mice, and that this expression is reduced by pretreatment with MMP-9 inhibitor in vivo. Recently, Yang et al. [58] demonstrated that JEV induced MMP-9 expression is mediated through ROS/c-Src/PDGFR/P13K/Akt/MAPKs-dependent activation of AP-1 signaling pathway in RBA-1 cells.

MMP-2 is constitutively expressed under normal conditions; however, its production is increased at the cell surface after binding to activated adhesion molecules. Rosenberg and others [42] have shown in an animal model that active MMP-2, which is constitutively expressed by several cell types in human and animal CSF, is also able to open the BBB. In the present study, MMP-2 was significantly higher as compared to controls. TH2 cells may help to induce MMP-2 secretion to some extent [35]. It is feasible that MMP-2 is also essential for restoring the integrity of the peripheral nervous system and for recovery from the disease. MMP-2 and MMP- 9 are structurally similar gelatinases that can each be activated by MMP-7 [55].

Several cytokines, including TNF-α, have been shown to increase MMP-7 expression and have been repeatedly linked to EAE and MS inflammation [13]. Study by Lillian A Buhler et al. [8] suggest that MMP-7 plays a role in the extravasation of immune cells during EAE.

Zymography was also performed to ascertain the gelatinase activities of MMP-2 and MMP-9 in sera following JEV infection. Zymography results showed that MMP-2 and MMP-9 activities were higher in virus infected groups as compared to control groups (Fig. 2a, b). The zymography data obtained in the sera are in concordance with the zymography data obtained in the CNS and in clinical specimens (CSF and serum) demonstrated in our previous published studies [46, 47], that CNS MMP-2 and MMP-9 activities were significantly higher in virus infected groups with disease progression and increased tissue pathology when compared with control groups and clinical study showed an increased CSF and serum concentration of MMP-9 in JEV-infected children compared to DC. The

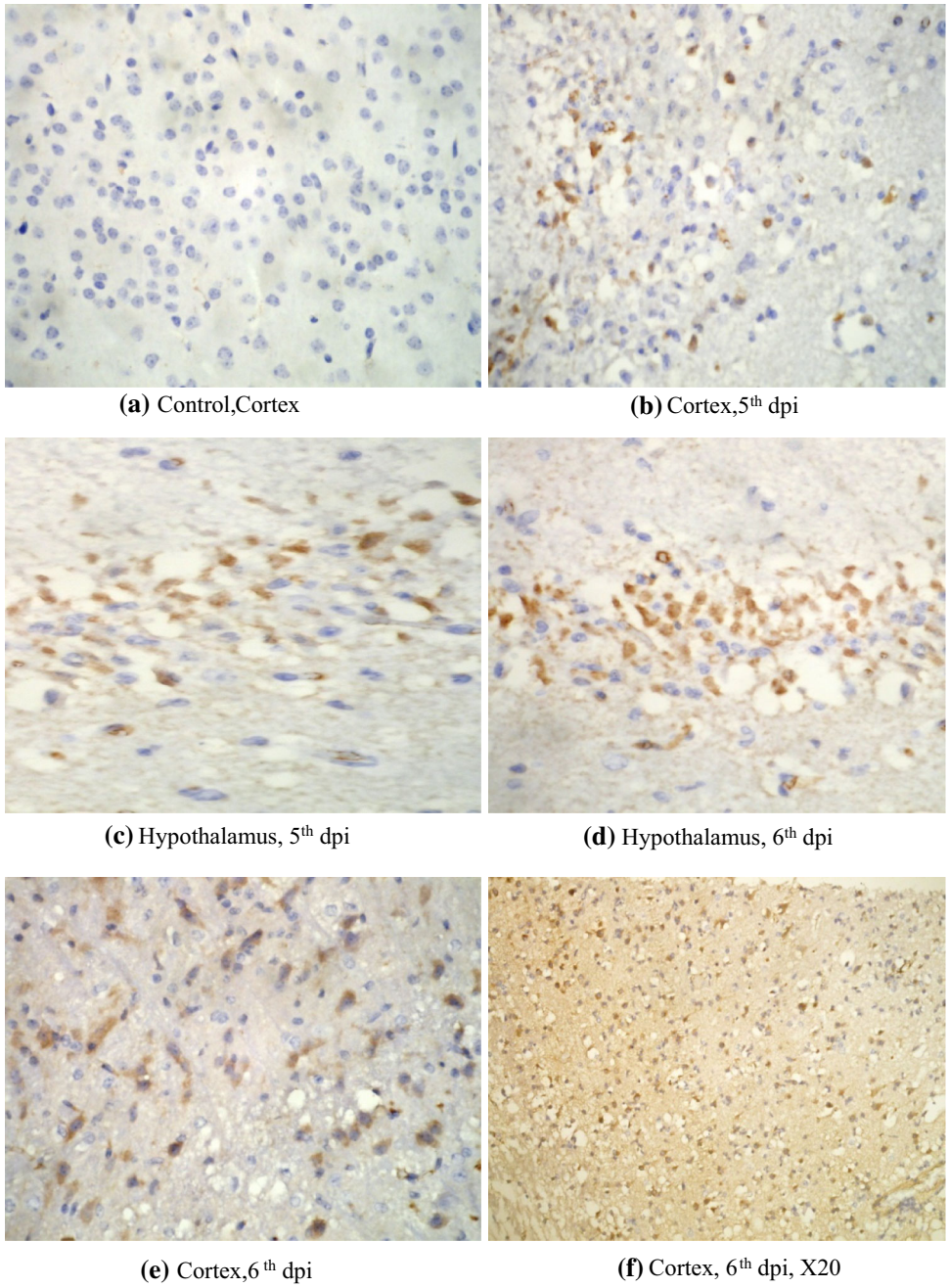

(a) Control,Cortex **(b)** Cortex,5th dpi

(c) Hypothalamus, 5th dpi **(d)** Hypothalamus, 6th dpi

(e) Cortex,6 th dpi **(f)** Cortex, 6th dpi, X20

Fig. 7 Photomicrograph showing presence of JEV antigen in cortex and hypothalamus region of BALB/c mouse brain infected with 3 × 106 pfu/ml of JEV(GP-78) at 5th and 6th dpi

zymographic data of CNS and CSF/serum raised the possibility that MMPs worsen the pathology in JEV infection. We also checked the integrity of BBB in an invivo model (Fig. 4) and found that its permeability was altered in the JEV infected mice group compared to control mouse.

In the present study, the mean serum concentration of TIMP-1 was increased significantly ($p < 0.001$) at all dpi compared to controls. Similarly, high levels of TIMP-3 was detected at 1 dpi and 5 dpi compared to controls ($p < 0.001$). Post hoc multiple comparison analysis between days in the virus infected group reveals that TIMP-1 and TIMP-3 were decreasing significantly ($p < 0.001$) with disease progression. This may be due to alterations of the cytokine milieu and other biologic factors that are major modulators of TIMP expression [6].

The present study also demonstrates that there is a very strong relationship between the production of MMPs and TIMPs (Table 2) in the virus infected group. The strong correlation between MMPs and TIMPs and viral load suggests a possible role of these immune mediators in immunopathogenesis of JEV infection.

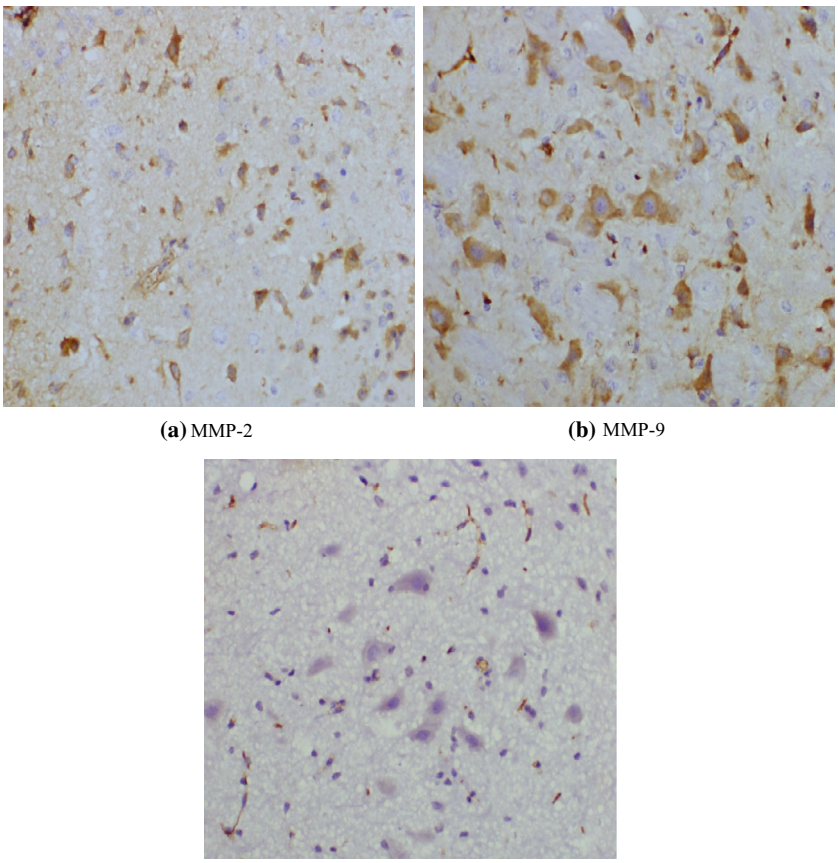

(a) MMP-2 **(b)** MMP-9

(c) Negative control

Fig. 8 Photomicrograph showing presence of **a** MMP-2 and **b** MMP-9 positive neurons in the cortex region of BALB/c mouse brain infected with 3 × 106 pfu/ml of JEV (GP-78) compared to negative control (**c**)

TIMPs can be co-expressed with MMPs, but some studies have shown a reciprocal regulation of their expression, which may depend on endogenously expressed (growth) factors and cytokines [15].

Many cytokines are produced by the immune system and are involved in cell signaling. Some cytokines are able to interact with the transcription of MMP and TIMP genes, or to alter their expression. This makes the effects of cytokines on MMPs and TIMPs very complex. Depending on the cell type, the same cytokine can either stimulate or inhibit MMP or TIMP expression. In general, TGF-β down-regulates MMP expression and up-regulates TIMP expression [34]. IL-10 inhibits MMP 9 expression in vitro, but induces TIMP-1 expression [23]. In contrast, IL-10 is able to inhibit the expression of other cytokines, and thus may counteract its own effects on MMP and TIMP expression [4, 12, 45, 48]. TNF-β stimulates the expression of several MMPs, and thus contributes to tissue degradation in inflammatory conditions [45]. Thus, in general, changes in cytokine expression may affect the MMP/TIMP balance in a cell-type dependent manner. Binding of the TIMPs to MMPs results in the efficient regulation of the protease activity and maintains the activation of MMPs in the extracellular space.

In summary, ELISA quantification of MMPs and TIMPs in serum appears to be sufficiently sensitive to provide a simple method for monitoring enzyme levels in JEV infection. The present study is the first, to our knowledge, to report serum measurements of MMP-2, MMP-7, MMP-9, TIMP-1 and TIMP-3 in JEV infection and to relate the

Table 2 Pearson's coefficient of correlation (r) between MMPs and TIMPs

Variables	r	Significance
MMP-2 *vs*		
MMP-7	0.87	0.001
MMP-9	0.88	0.99
TIMP-1	−0.92	0.001
TIMP-3	−0.86	0.98
MMP-7 *vs*		
MMP-9	0.99	0.001
TIMP-1	−0.89	0.94
TIMP-3	−0.76	0.001
MMP-9 *vs*		
TIMP-1	−0.92	0.001
TIMP-3	−0.80	0.99
TIMP-1 *vs*		
TIMP-3	0.97	0.001

levels to disease progression. We also provide preliminary evidence for a pattern of TIMP response in JEV infection distinct from that seen in acute inflammatory CNS conditions. Such findings suggest that MMPs may play a key role in the pathogenesis of JEV.

More studies on MMP/TIMP enzymatic system in animal models of JEV infection will be helpful in examining this issue and furthering our knowledge of the expression patterns of selected MMPs during the course of the disease. It is hoped that such insight may help in the design of specific MMP inhibitors that could be administered at critical checkpoints in the evolution of immune-mediated damage. Broad inhibition of MMPs reduced subarachnoid space inflammation and brain edema and partially prevented the breakdown of the BBB [50].

Acknowledgments We thank Dr. Sudhanshu Vrati from National Institute of Immunology, New Delhi, for providing the Japanese encephalitis virus strain GP-78 and PS cell line. We thank Dr. S. K. Mandal for his assistance with statistical analysis. This work was supported by a grant (No Immuno/18/11/13/2008-ECD-I) from the Indian Council of Medical Research, New Delhi, India.

References

1. Afonso PV, Ozden S, Prevost MC, Schmitt C, Seilhean D, Weksler B, et al. Human blood-brain barrier disruption by retroviral-infected lymphocytes: role of myosin light chain kinase in endothelial tight-junction disorganization. J Immunol. 2007;179(4):2576–83.
2. Balakrishnan A, Mishra AC. Immune response during acute Chandipura viral infection in experimentally infected susceptible mice. Virol J. 2008;5(1):121.
3. Basu A, Krady JK, Enterline JR, Levison SW. Transforming growth factor beta1 prevents IL-1beta-induced microglial activation, whereas TNFalpha- and IL-6-stimulated activation are not antagonized. Glia. 2002;40(1):109–20. doi:10.1002/glia.10118.
4. Birkedal-Hansen H. Role of cytokines and inflammatory mediators in tissue destruction. J Periodontal Res. 1993;28(6):500–10.
5. Biswas S, Kar S, Singh R, Chakraborty D, Vipat V, Raut C, et al. Immunomodulatory cytokines determine the outcome of Japanese encephalitis virus infection in mice. J Med Virol. 2010;82(2):304–10.
6. Bode W, Fernandez-Catalan C, Grams F, Gomis-Rüth FX, Nagase H, Tschesche H, et al. Insights into MMP-TIMP Interactions. Ann N Y Acad Sci. 1999;878(1):73–91.
7. Boven LA, Middel J, Verhoef J, De Groot CJ, Nottet HS. Monocyte infiltration is highly associated with loss of the tight junction protein zonula occludens in HIV-1-associated dementia. Neuropathol Appl Neurobiol. 2000;26(4):356–60.
8. Buhler L, Samara R, Guzman E, Wilson C, Krizanac-Bengez L, Janigro D, et al. Matrix metalloproteinase-7 facilitates immune access to the CNS in experimental autoimmune encephalomyelitis. BMC Neurosci. 2009;10(1):17.
9. Chen ZL, Strickland S. Neuronal death in the hippocampus is promoted by plasmin-catalyzed degradation of laminin. Cell. 1997;91(7):917–25.
10. Cosby SL, Brankin B. Measles virus infection of cerebral endothelial cells and effect on their adhesive properties. Vet Microbiol. 1995;44(2–4):135–9. doi:10.4049/jimmunol.179.4.2576
11. Dallasta LM, Pisarov LA, Esplen JE, Werley JV, Moses AV, Nelson JA, et al. Blood-brain barrier tight junction disruption in human immunodeficiency virus-1 encephalitis. Am J Pathol. 1999;155(6):1915–27. doi:10.1046/j.1365-2990.2000.00255.x.
12. de Waal Malefyt R, Abrams J, Bennett B, Figdor CG, de Vries JE. Interleukin 10 (IL-10) inhibits cytokine synthesis by human monocytes: an autoregulatory role of IL-10 produced by monocytes. J Exp Med. 1991;174(5):1209–20.
13. Ethell IM, Ethell DW. Matrix metalloproteinases in brain development and remodeling: synaptic functions and targets. J Neurosci Res. 2007;85(13):2813–23.
14. Ghosh D, Basu A. Japanese encephalitis—a pathological and clinical perspective. PLoS Negl Trop Dis. 2009;3(9):e437.
15. Gomez DE, Alonso DF, Yoshiji H, Thorgeirsson UP. Tissue inhibitors of metalloproteinases: structure, regulation and biological functions. Eur J Cell Biol. 1997;74(2):111.
16. Gralinski LE, Ashley SL, Dixon SD, Spindler KR. Mouse adenovirus type 1-induced breakdown of the blood–brain barrier. J Virol. 2009;83(18):9398–410. doi:10.1128/JVI.00954-09.
17. Gu Z, Kaul M, Yan B, Kridel SJ, Cui J, Strongin A, et al. S-nitrosylation of matrix metalloproteinases: signaling pathway to neuronal cell death. Science. 2002;297(5584):1186–90. doi:10.1126/science.1073634.
18. Hadass O, Tomlinson BN, Gooyit M, Chen S, Purdy JJ, Walker JM, et al. Selective inhibition of matrix metalloproteinase-9 attenuates secondary damage resulting from severe traumatic brain injury. PLoS One. 2013;8(10):e76904. doi:10.1016/S0092-8674(00)80483-3.
19. Hsieh HL, Yen MH, Jou MJ, Yang CM. Intracellular signalings underlying bradykinin-induced matrix metalloproteinase-9 expression in rat brain astrocyte-1. Cell Signal. 2004;16(10):1163–76.
20. Huber JD, Egleton RD, Davis TP. Molecular physiology and pathophysiology of tight junctions in the blood-brain barrier. Trends Neurosci. 2001;24(12):719–25. doi:10.1016/S0166-2236(00)02004-X
21. Ju SM, Song HY, Lee JA, Lee SJ, Choi SY, Park J. Extracellular HIV-1 Tat up-regulates expression of matrix metalloproteinase-9 via a MAPK-NF-κB dependent pathway in human astrocytes. Exp Mol Med. 2009;41(2):86.
22. Kieseier BC, Clements JM, Pischel HB, Wells GMA, Miller K, Gearing AJH, et al. Matrix metalloproteinases MMP-9 and MMP-7 are expressed in experimental autoimmune neuritis and the guillain-barr syndrome. Ann Neurol. 1998;43(4):427–34.
23. Lacraz S, Nicod LP, Chicheportiche R, Welgus HG, Dayer JM. IL-10 inhibits metalloproteinase and stimulates TIMP-1 production in human mononuclear phagocytes. J Clin Investig. 1995;96(5):2304.
24. Leppert D, Leib SL, Grygar C, Miller KM, Schaad UB, Hollander GA. Matrix metalloproteinase (MMP)-8 and MMP-9 in cerebrospinal fluid during bacterial meningitis: association with blood-brain barrier damage and neurological sequelae. Clin Infect Dis. 2000;31(1):80–4. doi:10.1086/313922.
25. Liu KJ, Rosenberg GA. Matrix metalloproteinases and free radicals in cerebral ischemia. Free Radic Biol Med. 2005;39(1):71–80. doi:10.1016/j.freeradbiomed.2005.03.033.
26. McGavern DB, Homann D, Oldstone M. T cells in the central nervous system: the delicate balance between viral clearance and disease. J Infect Dis. 2002;186(Supplement 2):S145.
27. Mikawa S, Kinouchi H, Kamii H, Gobbel GT, Chen SF, Carlson E, et al. Attenuation of acute and chronic damage following traumatic brain injury in copper, zinc-superoxide dismutase transgenic mice. J Neurosurg. 1996;85(5):885–91.
28. Mishra MK, Dutta K, Saheb SK, Basu A. Understanding the molecular mechanism of blood-brain barrier damage in an experimental model of Japanese encephalitis: correlation with

minocycline administration as a therapeutic agent. Neurochem Int. 2009;55(8):717–23. doi:10.1016/j.neuint.2009.07.006.
29. Mishra MK, Dutta K, Saheb SK, Basu A. Understanding the molecular mechanism of blood-brain barrier damage in an experimental model of Japanese encephalitis: correlation with minocycline administration as a therapeutic agent. Neurochem Int. 2009;55(8):717–23.
30. Missé D, Esteve PO, Renneboog B, Vidal M, Cerutti M, St Pierre Y, et al. HIV-1 glycoprotein 120 induces the MMP-9 cytopathogenic factor production that is abolished by inhibition of the p38 mitogen-activated protein kinase signaling pathway. Blood. 2001;98(3):541–7.
31. Morrey JD, Olsen AL, Siddharthan V, Motter NE, Wang H, Taro BS, et al. Increased blood–brain barrier permeability is not a primary determinant for lethality of West Nile virus infection in rodents. J Gen Virol. 2008;89(Pt 2):467–73. doi:10.1099/vir.0.83345-0.
32. Myint KS, Kipar A, Jarman RG, Gibbons RV, Perng GC, Flanagan B, et al. Neuropathogenesis of Japanese encephalitis in a primate model. PLoS Negl Trop Dis. 2014;8(8):e2980. doi:10.1371/journal.pntd.0002980.
33. Noble LJ, Donovan F, Igarashi T, Goussev S, Werb Z. Matrix metalloproteinases limit functional recovery after spinal cord injury by modulation of early vascular events. J Neurosci. 2002;22(17):7526–35.
34. Overall CM, Wrana JL, Sodek J. Independent regulation of collagenase, 72-kDa progelatinase, and metalloendoproteinase inhibitor expression in human fibroblasts by transforming growth factor-beta. J Biol Chem. 1989;264(3):1860.
35. Tsai HC, Shi MH, Lee SS, Wann SR, Tai MH, Chen YS. Expression of matrix metalloproteinases and their tissue inhibitors in the serum and cerebrospinal fluid of patients with meningitis. Clin Microbiol Infect. 2011;17(5):780–4. doi:10.1111/j.1469-0691.2010.03393.x.
36. Pachter JS, de Vries HE, Fabry Z. The blood-brain barrier and its role in immune privilege in the central nervous system. J Neuropathol Exp Neurol. 2003;62(6):593.
37. Paemen L, Olsson T, Söderström M, Damme J, Opdenakker G. Evaluation of gelatinases and IL-6 in the cerebrospinal fluid of patients with optic neuritis, multiple sclerosis and other inflammatory neurological diseases. Eur J Neurol. 1994;1(1):55–63.
38. Paul S, Ricour C, Sommereyns C, Sorgeloos F, Michiels T. Type I interferon response in the central nervous system. Biochimie. 2007;89(6–7):770–8. doi:10.1016/j.biochi.2007.02.009.
39. Robinson SC, Scott KA, Balkwill FR. Chemokine stimulation of monocyte matrix metalloproteinase-9 requires endogenous TNF-α. Eur J Immunol. 2002;32(2):404–12.
40. Rosenberg GA. Matrix metalloproteinases in brain injury. J Neurotrauma. 1995;12(5):833–42.
41. Rosenberg GA. Matrix metalloproteinases in neuroinflammation. Glia. 2002;39(3):279–91.
42. Rosenberg GA, Kornfeld M, Estrada E, Kelley RO, Liotta LA, Stetler-Stevenson WG. TIMP-2 reduces proteolytic opening of blood–brain barrier by type IV collagenase. Brain Res. 1992;576(2):203–7.
43. Saxena V, Mishra VK, Dhole TN. Evaluation of reverse-transcriptase PCR as a diagnostic tool to confirm Japanese encephalitis virus infection. Trans R Soc Trop Med Hyg. 2009;103(4):403–6.
44. Schafer A, Brooke CB, Whitmore AC, Johnston RE. The role of the blood–brain barrier during Venezuelan equine encephalitis virus infection. J Virol. 2011;85(20):10682–90. doi:10.1128/JVI.05032-11.
45. Shimizu K, Libby P, Mitchell RN. Local cytokine environments drive aneurysm formation in allografted aortas. Trends Cardiovasc Med. 2005;15(4):142–8.
46. Shukla V, Kumar Shakya A, Dhole T, Misra UK. Upregulated expression of matrix metalloproteinases and tissue inhibitors of matrix metalloproteinases in BALB/c mouse brain challenged with Japanese encephalitis virus. Neuroimmunomodulation. 2012;19(4):241–54.
47. Shukla V, Shakya AK, Dhole TN, Misra UK. Matrix metalloproteinases and their tissue inhibitors in serum and cerebrospinal fluid of children with Japanese encephalitis virus infection. Arch Virol. 2013;158(12):2561–75. doi:10.1007/s00705-013-1783-7.
48. Silacci P, Dayer JM, Desgeorges A, Peter R, Manueddu C, Guerne PA. Interleukin (IL)-6 and its soluble receptor induce TIMP-1 expression in synoviocytes and chondrocytes, and block IL-1-induced collagenolytic activity. J Biol Chem. 1998;273(22):13625.
49. Solomon T, Dung NM, Kneen R, Nisalak A, Vaughn DW, Farrar J, et al. Rapid diagnosis of Japanese encephalitis by using an immunoglobulin M dot enzyme immunoassay. J Clin Microbiol. 1998;36(7):2030–4.
50. Solorzano CC, Ksontini R, Pruitt JH, Auffenberg T, Tannahill C, Galardy RE, et al. A matrix metalloproteinase inhibitor prevents processing of tumor necrosis factor [alpha](TNF [alpha]) and abrogates endotoxin-induced lethality. Shock. 1997;7(6):427.
51. Tsai HC, Shi MH, Lee SSJ, Wann SR, Tai MH, Chen YS. Expression of matrix metalloproteinases and their tissue inhibitors in the serum and cerebrospinal fluid of patients with meningitis. Clin Microbiol Infect. 2011.
52. Tsai HC, Liu SF, Wu KS, Liu YC, Shi MH, Chen ER, et al. Dynamic changes of matrix metalloproteinase-9 in patients with Klebsiella pneumoniae meningitis. Inflammation. 2008;31(4):247–53.
53. Tsai HC, Chung LY, Chen ER, Liu YC, Lee SSJ, Chen YS, et al. Association of matrix metalloproteinase-9 and tissue inhibitors of metalloproteinase-4 in cerebrospinal fluid with blood–brain barrier dysfunction in patients with eosinophilic meningitis caused by Angiostrongylus cantonensis. Am J Trop Med Hyg. 2008;78(1):20–7.
54. Tung WH, Tsai HW, Lee I, Hsieh HL, Chen WJ, Chen YL, et al. Japanese encephalitis virus induces matrix metalloproteinase-9 in rat brain astrocytes via NF-κB signalling dependent on MAPKs and reactive oxygen species. Br J Pharmacol. 2010;161(7):1566–83.
55. Von Bredow DC, Cress AE, Howard EW, Bowden GT, Nagle RB. Activation of gelatinase-tissue-inhibitors-of-metalloproteinase complexes by matrilysin. Biochem J. 1998;331(Pt 3):965.
56. Wang T, Town T, Alexopoulou L, Anderson JF, Fikrig E, Flavell RA. Toll-like receptor 3 mediates West Nile virus entry into the brain causing lethal encephalitis. Nat Med. 2004;10(12):1366–73. doi:10.1038/nm1140.
57. Wu CY, Hsieh HL, Jou MJ, Yang CM. Involvement of p42/p44 MAPK, p38 MAPK, JNK and nuclear factor-kappa B in interleukin-1β-induced matrix metalloproteinase-9 expression in rat brain astrocytes. J Neurochem. 2004;90(6):1477–88.
58. Yang CM, Lin CC, Lee IT, Lin YH, Chen WJ, Jou MJ, et al. Japanese encephalitis virus induces matrix metalloproteinase-9 expression via a ROS/c-Src/PDGFR/PI3K/Akt/MAPKs-dependent AP-1 pathway in rat brain astrocytes. J Neuroinflammation. 2012;9(1):12.
59. Yong VW, Power C, Forsyth P, Edwards DR. Metalloproteinases in biology and pathology of the nervous system. Nat Rev Neurosci. 2001;2(7):502–11.
60. Yu F, Kamada H, Niizuma K, Endo H, Chan PH. Induction of mmp-9 expression and endothelial injury by oxidative stress after spinal cord injury. J Neurotrauma. 2008;25(3):184–95. doi:10.1089/neu.2007.0438.
61. Zhang H, Adwanikar H, Werb Z, Noble-Haeusslein LJ. Matrix metalloproteinases and neurotrauma: evolving roles in injury and reparative processes. Neuroscientist. 2010;16(2):156–70. doi:10.1177/1073858409355830.